Crossing of conduction- and valence-subband Landau levels in an inverted HgTe/CdTe quantum well

M. Schultz and U. Merkt
Institut für Angewandte Physik und Zentrum für Mikrostrukturforschung, Universität Hamburg, Jungiusstrasse 11, 20355 Hamburg, Germany

A. Sonntag and U. Rössler
Institut für Theoretische Physik, Universität Regensburg, Universitätsstrasse 31, 93040 Regensburg, Germany

R. Winkler
Institut für Technische Physik III, Universität Erlangen-Nürnberg, Staudtstrasse 7, 91058 Erlangen, Germany

T. Colin, P. Helgesen, T. Skauli, and S. Løvold
Norwegian Defence Research Establishment, Division for Electronics, P.O. Box 25, 2007 Kjeller, Norway
(Received 11 December 1997)

In the inverted-band regime of HgTe/CdTe quantum wells, the lowest Landau level of the lowest conduction subband and the highest Landau level of the topmost valence subband are predicted to cross at a critical magnetic field B_c. We study this crossing experimentally with far-infrared Fourier-transform spectroscopy in a gated HgTe/CdTe quantum well with tunable electron density. The crossing point is identified by a characteristic exchange of oscillator strength between the two transitions involved, one being a cyclotron resonance, the other an intersubband resonance. The experimental resonance positions, the oscillator strengths as well as the value of B_c, are in good agreement with theoretical results of a 6×6 $\mathbf{k}\cdot\mathbf{p}$ model evaluated for the [211] growth direction. [S0163-1829(98)07515-8]

Heterostructures of HgTe and CdTe are of type III combining a positive band gap semiconductor (CdTe) and a negative band gap semimetal (HgTe) with gaps formed between states of Γ_8 and Γ_6 symmetry. Layered quantum structures of these materials have attracted interest due to the possible formation of interface states and a quasizero gap system,[1,2] which allows for a double semiconductor-semimetal-semiconductor transition.[3] The valence-band offset, being the crucial parameter of this system, has been a point of controversies.[3–7] While most of the work on this system has been devoted to superlattices,[8] in this paper we report on a gated HgTe single quantum well (QW) with tunable electron density. This structure allows us to study the filling factor dependence of its Landau levels at fixed magnetic field. Depending on their thicknesses, single HgTe QW's between CdTe barriers can exist in two distinct regimes. For small widths ($L_z \lesssim 70$ Å) (Ref. 6) and thus larger subband separations, an open gap is formed between an $M = \pm 3/2$ heavy-hole subband (HH1) and an electronlike light-particle subband ($E1$) whose states are a mixture of the Γ_6 and the Γ_8 light-hole bulk states (angular momentum $M = \pm 1/2$). This corresponds to the normal regime. For increasing well widths, the $E1$ subband falls below the topmost HH subbands and takes on holelike character, while the HH1 subband becomes electronlike. Such QW's are in the inverted-band regime.[3] The dispersion of the subbands, which indicate the electron or hole character, are determined by coupling heavy-hole to light-particle states at finite in-plane wave vectors $k_\parallel$. Our notation for labeling the subbands corresponds to the dominant spinor component M at $k_\parallel = 0$.

A quantizing magnetic field applied along the growth direction of the QW structure uncovers the mixed nature of the HH1 subband in the inverted-band regime (see Fig. 1). The lowest Landau level $n_L = 0$ contains pure HH ($M = -3/2$) states which do not mix with the light-particle ($M = \pm 1/2$) states.[9] Accordingly, this level lowers its energy linearly with increasing magnetic field, while all other Landau levels of the HH1 subband rise in energy with magnetic field due to the coupling with light-particle states. Thus they show an electron-like character. This unusual behavior in inverted-band QW's together with the peculiar dispersion of the $n_L = 2$ level from the topmost valence subband (HH2) leads

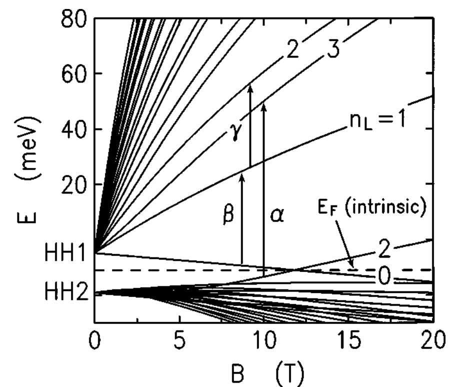

FIG. 1. Calculated Landau levels for a HgTe/CdTe QW in the inverted-band regime of width 122 Å with the intrinsic Fermi energy marked by a dashed line. The cyclotron resonance (CR) transitions β and γ as well as the intersubband resonance (ISR) transition α are indicated by arrows.

0163-1829/98/57(23)/14772(4)/$15.00 © 1998 The American Physical Society

TABLE I. **k·p** band parameters for HgTe and CdTe taken from Refs. 18,19.

	E_0 (eV)	P (eVÅ)	m^*/m_0	g^*	γ_1	γ_2	γ_3	κ
HgTe	−0.300	8.31	−0.028	41.0	−15.6	−9.6	−8.6	−11.2
CdTe	1.606	8.31	0.090	−1.77	4.14	1.09	1.62	0.457

to a crossing of conduction- and valence-subband states at a critical value B_c of the magnetic field (see Fig. 1). A corresponding fan chart has been reported earlier for semimetallic and inverted-band HgTe/CdTe superlattices.[10,11] Here, we describe magneto-optical measurements at a fixed temperature that prove the existence of this crossing phenomenon in an inverted single QW.

The sample was grown by molecular-beam epitaxy (MBE) on a CdZnTe (211)B substrate.[12] Its layer sequence is as follows: a 1825 Å CdTe buffer, a 122 Å HgTe QW, and a 425 Å CdTe cap layer. The CdTe layers may contain up to 5% Hg. From the single QW sample, a metal-oxide-semiconductor (MOS) capacitor was fabricated with a 1300-Å-thick SiO_2 insulator and a semitransparent 75-Å-thin NiCr gate of 3 mm in diameter.[13] Contacts were soldered at the edges of the sample to allow magnetocapacitance measurements from which the electron density $n_s = 1.25\times10^{11}$ cm^{-2} V$^{-1}(V_g - V_{\rm th})$ as a function of gate voltage V_g could be deduced. The magnetocapacitance measurements as well as cyclotron resonance (CR) at low magnetic fields ($B \leqslant 3$T) yield a threshold of $V_{\rm th} = 3.7$ V for the induction of electrons into the conduction subband. In the spectroscopic experiments the relative change of transmittance $-\Delta T/T_{\rm ref} = -[T(V_g) - T_{\rm ref}]/T_{\rm ref}$ with the reference spectra $T_{\rm ref}$ taken at $V_g = -4$ V is recorded with a Fourier-transform spectrometer in the spectral range 20–700 cm^{-1} using unpolarized light. To eliminate interference effects, the back of the sample was wedged at an angle of about 3°. The magnetic field is applied in growth direction and the measurements are performed in Faraday geometry at a temperature of 5 K. From the CR measurements at low magnetic fields an effective mass of $m^* = 0.024 m_e$ and a mobility of $\mu = 30\,000$ cm^2 V^{-1} s^{-1} are deduced for an electron density of $n_s = 2.9 \times 10^{11}$ cm^{-2}.

For the calculation of Landau levels (Fig. 1) we employ a 6×6 **k·p** model including the fourfold Γ_8 and the twofold Γ_6 states of the bulk-band structure of HgTe and CdTe.[14–16] We use the bulk-band parameters in Table I. Best agreement with experiment is obtained using a valence-band offset of 700 meV. This value is of the same order as the room-temperature value of 730–850 meV obtained by Yoo *et al.*[5] The calculations are performed in the axial approximation for growth direction [211].[17] Due to the small carrier densities self-consistent corrections did not change the potential profile significantly. Taking the split-off valence band Γ_7 explicitly into account (as done in Ref. 7) did not change our results either, which is a consequence of the large spin-orbit splitting of about 1 eV in both HgTe and CdTe.

The Landau levels shown in Fig. 1 evolve from HH states at −4.8 meV (HH1) and −19.1 meV (HH2). In the axial model they can be classified by $n_L = F_z + 1/2$ with F_z the z component of the total angular momentum.[14] In general these levels result from mixing of Landau oscillators belonging to different spinor components M of the multicomponent envelope function and show a nonlinear dependence on magnetic field.[16] However, the lowest HH1 Landau level with quantum number $n_L = 0$ is completely decoupled from the other states (it contains pure $M = -3/2$ states), and its energy decreases linearly in B.[9] The most decisive feature of Fig. 1 is the crossing of this level with the (HH2,$n_L = 2$) Landau level at $B_c = 12$ T. For $B \gtrsim 5$T the energy of the latter level also varies almost linearly with B. But unlike the (HH1,$n_L = 0$) level at B_c it is a strong mixture of the $M = -3/2$ and $M = \pm 1/2$ spinor components.

As mentioned before for a QW in the inverted-band regime the gap opens between the HH1 and the next lower subband, which in our sample is the HH2 subband. Thus the Fermi level E_F for the unbiased (intrinsic) QW is as indicated in Fig. 1: At zero temperature all states below E_F are occupied, all states above E_F are empty. In our calculations this position of the intrinsic Fermi energy is confirmed by varying the gap parameter E_0 of the well material: Starting from a subband structure with an open gap ($E_0 > 0$) the lowest-lying light-particle electron subband falls below the topmost hole subbands when the gap parameter is decreased to the actual value $E_0 = -300$ meV in HgTe. Then it becomes holelike while the topmost HH subband becomes electronlike. Experimentally the intrinsic situation is realized at the threshold voltage $V_{\rm th}$.

For unpolarized light, dipole transitions between Landau levels follow the selection rule $\Delta n_L = \pm 1$. The intensity depends on their occupation and their dipole matrix elements.[16] Around the intrinsic Fermi energy for $\Delta n_L = +1$ two transitions are possible which are marked by arrows in Fig. 1. The transition (HH1,$n_L = 0$)→(HH1,$n_L = 1$) is a CR transition between Landau levels evolving from the same subband. It shows up at $B > B_c$. The transition (HH2,$n_L = 2$)→(HH1,$n_L = 3$) is an intersubband resonance (ISR) which appears for $B < B_c$. In our experiment we establish a situation with low densities of extrinsic carriers, where up to B_c the Fermi energy lies in the (HH1,$n_L = 0$) level and in the (HH2,$n_L = 2$) level for higher magnetic fields. Accordingly, the intensity of the CR should increase above the critical point B_c while the ISR should become weaker. For unpolarized light the transitions with $\Delta n_L = -1$ are less important (see below).

In our gated sample the model can be tested by varying the magnetic field at a constant gate voltage or by varying the gate voltage at a constant magnetic field. Figure 2 shows the absorption of the sample at $B = 10$ T for different gate voltages or filling factors $\nu = n_s h/eB$. At the gate voltage $V_g = 4$ V, which is slightly above the threshold deduced from CR and magnetocapacitance data in low magnetic fields, a strong transition α at 550 cm^{-1} and a weaker transition β at 375 cm^{-1} are visible which we identify as the ISR transition (HH2,$n_L = 2$)→(HH1,$n_L = 3$) and the CR transition (HH1,$n_L = 0$)→(HH1,$n_L = 1$), respectively. With increasing

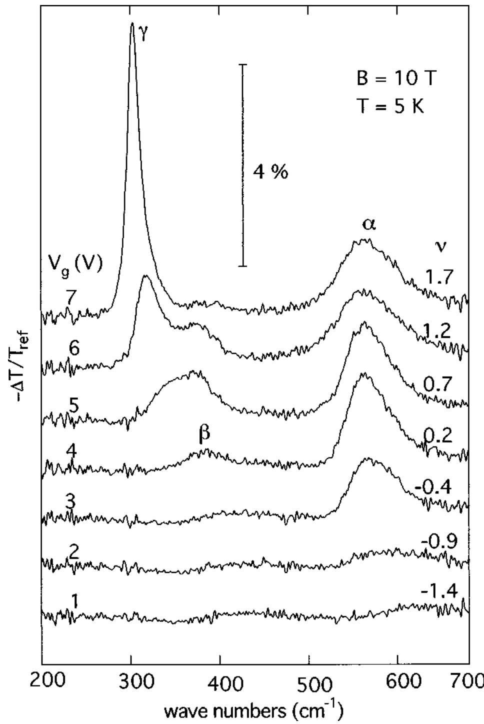

FIG. 2. Normalized transmittance spectra of a 122-Å-thin HgTe QW for various gate voltages V_g or filling factors ν in a fixed magnetic field $B=10$ T. The spectra show the CR transitions β and γ as well as the ISR transition α.

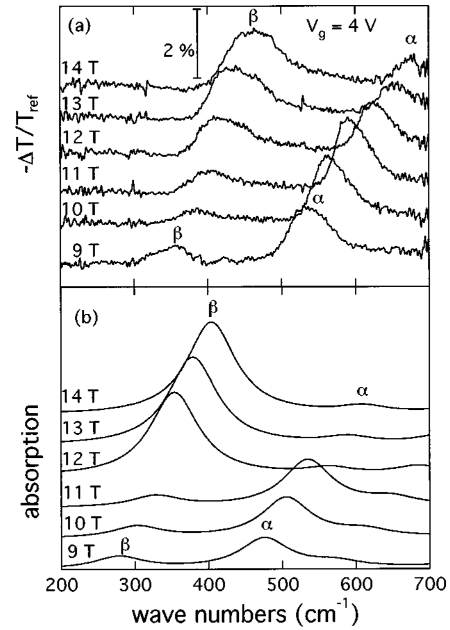

FIG. 3. (a) Experimental and (b) theoretical spectra for various magnetic fields at a fixed electron density $n_s=4\times10^{10}$ cm^{-2}. Note the exchange of oscillator strength between the $0\rightarrow1$ CR transition β and the $2\rightarrow3$ ISR transition α.

gate voltage the CR β gains oscillator strength and at a filling factor of $\nu=1.2$ a third transition γ can be found at 320 cm^{-1}. We identify γ as the $1\rightarrow2$ CR transition in the conduction subband HH1. The resonance γ is narrower than the other two resonances. This we interpret to be due to a better screening of impurities at higher electron densities. The resonance γ is comparable to the generic CR of narrow-gap semiconductors with spin-split Landau levels. The resonance β, on the other hand, which involves the purely $M=-3/2$ Landau level (HH1,$n_L=0$), is specific to the inverted-band regime. At the filling factor $\nu=1.7$ the transition β has almost vanished. This can be explained by the filling of the final level $n_L=1$ with electrons. Lowering the gate voltage under the threshold leads to the disappearance of the ISR transition α at $V_g=2$ V. This voltage is equivalent to a filling factor of $\nu=-0.9$. By negative filling factors we denote depopulation of the Landau levels of the valence subbands. The disappearance of resonance α can be explained as follows: the Landau level $n_L=2$ is the highest-lying Landau level of the valence subband HH2 at higher magnetic fields (see Fig. 1). Therefore this level will be totally depleted at a filling factor $\nu=-1$. As a result, the intersubband transition α disappears. We like to add here, that when states of the valence subband HH2 start to become depopulated, we detect additional absorption in the region of wave numbers 100 cm^{-1} (not shown in Fig. 2). This we attribute to hole CR within the HH2 subband. The polarization dependence of this signal is in fact consistent with the one for hole transitions, i.e., it is stronger for left-hand circularly polarized light.

Having thus shown the consistency between the experimental spectra of Fig. 2 and the theoretical results depicted in Fig. 1 we investigate now the crossing feature of the Landau levels (HH1,$n_L=0$) and (HH2,$n_L=2$). For a gate voltage of $V_g=4$ V we have an electron density of 4×10^{10} cm^{-2} in the conduction subband HH1 and a filling factor $\nu=0.2$ at $B=10$ T (see Fig. 2). Figure 3(a) shows the absorption spectra for magnetic fields in the range $B=9$ to 14 T. It depicts a clear evolution of the oscillator strength of the two peaks β and α. At $B=9$ T there is a weak CR β at 350 cm^{-1} and a strong ISR α at 550 cm^{-1}. With increasing magnetic field the CR gains oscillator strength at the expense of the ISR. Between 12 T and 13 T the intensities equal each other. At the highest magnetic field $B=14$ T the CR dominates the spectrum and the ISR transition has become weak. This exchange of oscillator strength between CR and ISR can be directly related to the crossing feature of the Landau levels $n_L=0$ and $n_L=2$ in Fig. 1, and thus to the inverted-band regime of the HgTe QW. At $B<12$ T the lowest level $n_L=0$ of the conduction subband HH1 is only partially filled at the gate voltage $V_g=4$ V and CR is very weak. At a critical field between 12 T and 13 T the Landau level $n_L=0$ of the conduction subband HH1 crosses the Landau level $n_L=2$ of the valence subband HH2. Then, both levels are evenly populated with electrons. As the corresponding dipole matrix elements are comparable, the CR and ISR are equally strong. At higher fields $B>13$ T the Landau level $n_L=0$ of HH1 becomes the topmost valence level which is completely filled at $V_g=4$ V, while the Landau level $n_L=2$ of HH2 takes the role of the lowest conduction level which is only partially filled. For these values of B and V_g, almost all of the oscillator strength is in the CR. Hence, the change of oscillator strength between ISR and CR can be directly attributed to the redistribution of electrons between the conduction and valence subbands HH1 and HH2 as a consequence of the crossing of their Landau levels in a magnetic field.

In order to confirm the interpretation of Fig. 3(a), we have calculated the absorption spectra based on the Landau levels of Fig. 1 and the magnetic-field-dependent filling factors for the carrier density $n_s = 4.0 \times 10^{10}$ cm^{-2}. The calculations follow the concept outlined in Ref. 16. A phenomenological constant broadening of 5 meV has been assumed. In accordance with the normalization of the experimental spectra only those transitions were taken into account for which the initial states are unoccupied at $V_g = -4$ V. Transitions which are allowed at $V_g = -4$ V but forbidden at $V_g = 4$ V [so that they give a negative contribution to the spectra in Fig. 3(a)] turned out to be negligible. The results in Fig. 3(b) are in good agreement with the experimental spectra in Fig. 3(a), with respect to the oscillator strengths and to the spectral positions. In the calculated spectra the exchange of oscillator strength around B_c is more pronounced, presumably due to the assumption of zero temperature. In Fig. 3(b) the peak α consists of two transitions, $(\mathrm{HH2}, n_L = 2) \rightarrow (\mathrm{HH1}, n_L = 3)$, and at a slightly higher energy and with a smaller oscillator strength, the transition $(\mathrm{HH2}, n_L = 3) \rightarrow (\mathrm{HH1}, n_L = 2)$. The latter is the only transition with $\Delta n_L = -1$ in the calculated spectra of Fig. 3(b).

We found that if we take into account that the barriers may contain some Hg we need a *smaller* offset in our calculation (610 meV for 5% Hg). We could have tried to further improve the agreement between experiment and theory by varying some model parameters other than the valence band offset. Truchseß *et al.* developed a new set of $\mathbf{k} \cdot \mathbf{p}$ parameters for HgTe and CdTe (Ref. 7) in order to interpret their experiments on HgTe/CdTe quantum structures. However, their CdTe parameters differ considerably from values which have been obtained in various bulk experiments.[18] On the other hand, due to a smaller database[19] band parameters for HgTe are less reliable than those for CdTe.

In conclusion, we have demonstrated a peculiar feature occurring in HgTe/CdTe QW's in the inverted-band regime: a crossing between Landau levels evolving from the lowest conduction and the highest valence subbands in strong magnetic fields. Comparison of far-infrared spectra taken of a QW with low carrier concentration with calculated Landau levels and absorption spectra obtained from a 6×6 $\mathbf{k} \cdot \mathbf{p}$ model allow us to ascribe this feature to the type III character of the HgTe/CdTe heterostructure system. Best agreement between theory and experiment was obtained using a valence-band offset of 700 meV.

We thank the Deutsche Forschungsgemeinschaft for financial support.

[1] Y. R. Lin-Liu and L. J. Sham, Phys. Rev. B **32**, 5561 (1985).

[2] Y. Guldner, G. Bastard, J. P. Vieren, M. Voos, J. P. Faurie, and A. Million, Phys. Rev. Lett. **51**, 907 (1983).

[3] N. F. Johnson, P. M. Hui, and H. Ehrenreich, Phys. Rev. Lett. **61**, 1993 (1988).

[4] J. M. Berroir, Y. Guldner, J. P. Vieren, M. Voos, and J. P. Faurie, Phys. Rev. B **34**, 891 (1986).

[5] K. H. Yoo, R. L. Aggarwal, L. R. Ram-Mohan, and O. K. Wu, J. Vac. Sci. Technol. A **8**, 1194 (1990).

[6] Z. Yang, Z. Yu, Y. Lansari, S. Hwang, J. W. Cook, Jr., and J. F. Schetzina, Phys. Rev. B **49**, 8096 (1994).

[7] M. von Truchseß, V. Latussek, F. Goschenhofer, C. R. Becker, G. Landwehr, E. Batke, R. Sizmann, and P. Helgesen, Phys. Rev. B **51**, 17 618 (1995).

[8] J. R. Meyer, C. A. Hoffman, and F. J. Bartoli, in *II-VI Semiconductor Compounds*, edited by M. Jain (World Scientific, Singapore, 1993), p. 301, and references therein.

[9] F. Ancilotto, A. Fasolino, and J. C. Maan, Phys. Rev. B **38**, 1788 (1988).

[10] J. R. Meyer, R. J. Wagner, F. J. Bartoli, C. A. Hoffman, M. Dobrowolska, T. Wojtowicz, J. K. Furdyna, and L. R. Ram-Mohan, Phys. Rev. B **42**, 9050 (1990).

[11] M. von Truchsess, A. Pfeuffer-Jeschke, V. Latussek, C. R. Becker, and E. Batke, in *High Magnetic Fields in the Physics of Semiconductors II*, edited by G. Landwehr and W. Ossau (World Scientific, Singapore, 1997), Vol. 2, p. 813.

[12] T. Colin, D. Minsås, S. Gjøen, R. Sizmann, and S. Løvold, in *Compound Semiconductor Epitaxy*, edited by C. W. Tu, L. A. Kolodziejski, and V. R. McCrary, MRS Symposia Proceedings No. 340 (Materials Research Society, Pittsburgh, 1994), p. 575.

[13] M. Schultz, F. Heinrichs, U. Merkt, T. Colin, T. Skauli, and S. Lovold, Semicond. Sci. Technol. **11**, 1168 (1996).

[14] H. R. Trebin, U. Rössler, and R. Ranvaud, Phys. Rev. B **20**, 686 (1979).

[15] R. Winkler and U. Rössler, Phys. Rev. B **48**, 8918 (1993); Surf. Sci. **305**, 295 (1994).

[16] R. Winkler, M. Merkler, T. Darnhofer, and U. Rössler, Phys. Rev. B **53**, 10 858 (1996).

[17] Following the approach outlined in Ref. 35 of K. Suzuki and J. C. Hensel, Phys. Rev. B **9**, 4184 (1974), it turns out that for the axial approximation for growth direction [211] the prefactors in the $\mathbf{k} \cdot \mathbf{p}$ model are the same as those for [110]. The latter are given in Table VI of Ref. 14.

[18] T. Friedrich, J. Kraus, M. Meininger, G. Schaack, and W. O. G. Schmitt, J. Phys.: Condens. Matter **6**, 4307 (1994).

[19] *Semiconductors. Intrinsic Properties of Group IV Elements and III-V, II-VI, and I-VII Compounds*, edited by O. Madelung and M. Schulz, Landolt-Börnstein, New Series, Group III, Vol. 22, Pt. a (Springer, Berlin, 1987).